Relativistic ponderomotive force, uphill acceleration, and transition to chaos

D. Bauer, P. Mulser, and W.-H. Steeb*
Theoretical Quantum Electronics (TQE), Technische Hochschule Darmstadt, Hochschulstr. 4A, D-64289 Darmstadt, FRG
(Reprint of Phys. Rev. Lett. **75** 4622 (1995))

Abstract

Starting from a covariant cycle-averaged Lagrangian the relativistic oscillation center equation of motion of a point charge is deduced and analytical formulae for the ponderomotive force in a travelling wave of arbitrary strength are presented. It is further shown that the ponderomotive forces for transverse and longitudinal waves are different; in the latter, uphill acceleration can occur. In a standing wave there exists a threshold intensity above which, owing to transition to chaos, the secular motion can no longer be described by a regular ponderomotive force.

PACS number(s): 52.20.Dq,05.45.+b,52.35.Mw,52.60.+h

Typeset using REVTEX

A so-called ponderomotive potential Φ_p is induced by the oscillatory motion of a free charge. This potential plays a dominant role in atomic physics (e.g. multiphoton ionization) and laser plasma dynamics (e.g. parametric instabilities, self focusing, beat wave accelerator, fast ignitor [1]). It was shown independently by several authors [2] that for a monochromatic electromagnetic field of arbitrary space dependence,

$$\boldsymbol{E}(\boldsymbol{x}, t) = \Re \hat{\boldsymbol{E}}(\boldsymbol{x}) e^{-i\omega t}, \tag{1}$$

the oscillation center dynamics of a charge q is governed by the so-called ponderomotive force $\boldsymbol{f}_p$,

$$\boldsymbol{f}_p = -\frac{q^2}{4m\omega^2} \boldsymbol{\nabla}(\hat{\boldsymbol{E}} \cdot \hat{\boldsymbol{E}}^*). \tag{2}$$

Eq.(2) was obtained from a first order perturbation analysis of the Lorentz force [3] around the oscillation center and is therefore subject to the usual smallness constraints of certain parameters. In order to obtain some weak generalizations of this expression, a variety of different approaches was chosen [4–6]. Again, they are characterized by (i) a perturbation analysis of momentum, (ii) harmonic fields of type Eq.(1), and (iii) a small ratio of oscillation amplitude to wavelength λ. Recently, however, in connection with the existence of new lasers capabable of delivering ultrahigh irradiance a real need for relativistic expressions for $\boldsymbol{f}_p$, not bound by such limits, has arisen. One of the aims of this letter is to show under which conditions $\boldsymbol{f}_p$ exists and what forms it assumes.

The relativistic Lagrangian $L(\boldsymbol{x}, \boldsymbol{v}, t), \;\; \boldsymbol{v} = d\boldsymbol{x}/dt$, of a charge q in an arbitrary electromagnetic field $\boldsymbol{E} = -\boldsymbol{\nabla}\Phi - \partial \boldsymbol{A}/\partial t$ is given by

$$L(\boldsymbol{x}, \boldsymbol{v}, t) = -\frac{mc^2}{\gamma} + q\boldsymbol{v} \cdot \boldsymbol{A} - q\Phi; \;\; \gamma = (1 - v^2/c^2)^{-1/2}. \tag{3}$$

When an oscillation center exists, the transformation to action-angle variables $S = S(\boldsymbol{x}, t), \;\; \eta = \eta(\boldsymbol{x}, t)$ is possible (e.g. $\eta = \boldsymbol{k} \cdot \boldsymbol{x} - \omega t$ in the case of a travelling monochromatic wave). The action S and the angle η are both Lorentz-invariant. The motion of the particle is governed by Hamilton's principle,

$$\delta S = \delta \int_{\eta_1}^{\eta_2} L(\boldsymbol{x}(\eta), \boldsymbol{v}(\eta), t(\eta)) \frac{dt}{d\eta} d\eta = 0. \tag{4}$$

From the Lorentz invariance of S and η follows that the Lagrangian $\mathcal{L}(\eta) = L(d\eta/dt)^{-1}$ is invariant with respect to a change of the inertial reference system. Assuming that η is normalized to 2π for one full cycle or period of motion, the cycle-averaged Lagrangean $\mathcal{L}_0$,

$$\mathcal{L}_0(\eta) = \frac{1}{2\pi} \int_{\eta}^{\eta+2\pi} \mathcal{L}(\eta') d\eta', \tag{5}$$

depending only on the secular (i.e. oscillation center) coordinates $\boldsymbol{x}_0, \boldsymbol{v}_0$ through η is defined. The oscillation center motion is governed by the Lagrange equations of motion,

$$\frac{d}{dt} \frac{\partial L_0}{\partial \boldsymbol{v}_0} - \frac{\partial L_0}{\partial \boldsymbol{x}_0} = 0, \tag{6}$$

with $L_0 = \mathcal{L}_0 d\eta/dt$. To demonstrate this assertion we prove the following
Theorem: The validity of Eq.(4) implies

$$\delta \int_{\eta_i}^{\eta_f} \mathcal{L}_0(\eta) d\eta = o(N^{-1}). \tag{7}$$

Thereby $N = (\eta_f - \eta_i)/2\pi$ is the number of cycles over which $\mathcal{L}_0$ undergoes an essential change. The symbol $o(N^{-1})$ means: "vanishes at least with order $1/N$".
Proof: Let the variation be an arbitrary piecewise continuous function $\Delta(\eta)$. The n-th cycle starts at $\eta = \eta_n$, at which for brevity we use the symbols $\Delta_n = \Delta(\eta_n)$, $\partial\mathcal{L}_0/\partial\eta_n = (\partial\mathcal{L}_0/\partial\eta)_{\eta=\eta_n}$. If the same quantities refer to an intermediate point $\eta \le \eta_a \le \eta_n + 2\pi$ we write Δ_a and $\partial\mathcal{L}_0/\partial\eta_a$ and omit the index n for the interval. In leading order holds:

$$\begin{aligned}
&\left|\delta \int_{\eta_i}^{\eta_f} \mathcal{L}_0 d\eta\right| = \left|\int_{\eta_i}^{\eta_f} \delta(\mathcal{L}_0 - \mathcal{L}) d\eta\right| \\
&= \left|\int_{\eta_i}^{\eta_f} \left[\mathcal{L}_0(\eta+\Delta) - \mathcal{L}(\eta+\Delta)\right] d\eta - \int_{\eta_i}^{\eta_f} \left[\mathcal{L}_0(\eta) - \mathcal{L}(\eta)\right] d\eta\right| \\
&\le \sum_n \left|\int_{\eta_n}^{\eta_n+2\pi} \mathcal{L}_0(\eta+\Delta) d\eta - 2\pi\mathcal{L}_0(\eta_n+\Delta_n) - \left[\int_{\eta_n}^{\eta_n+2\pi} \mathcal{L}_0(\eta) d\eta - 2\pi\mathcal{L}_0(\eta_n)\right]\right| \\
&= \sum_n \left|\int_{\eta_n}^{\eta_n+2\pi} \frac{\partial\mathcal{L}_0}{\partial\eta_n}\Delta(\eta) d\eta - 2\pi\frac{\partial\mathcal{L}_0}{\partial\eta_n}\Delta_n\right| = 2\pi\sum_n \left|\frac{\partial\mathcal{L}_0}{\partial\eta_a}\Delta_a - \frac{\partial\mathcal{L}_0}{\partial\eta_n}\Delta_n\right|.
\end{aligned}$$

In the last step the mean value theorem is used. The function $\Delta(\eta)$ is arbitrary. Therefore at $\eta = \eta_n$ $\Delta_n = \Delta_a$ can be chosen now without affecting Δ_a. With this substitution the leading order gives the result

$$\left|\delta \int_{\eta_i}^{\eta_f} \mathcal{L}_0 d\eta\right| \le (2\pi)^2 \sum_n \left|\frac{\partial^2\mathcal{L}_0}{\partial\eta_n^2}\Delta_a\right| \le (2\pi)^2 N \max\left|\frac{\partial^2\mathcal{L}_0}{\partial\eta_n^2}\right| \times \max|\Delta_a|.$$

In this last step it is essential that $\partial\mathcal{L}_0/\partial\eta$ is a smooth function (in contrast to Δ which is generally not). Now, $N = \min \frac{1}{2\pi}|\mathcal{L}_{0\,\max}/(\partial\mathcal{L}_0/\partial\eta_n)|$ is chosen, i.e. over N cycles $\mathcal{L}_{0\,\max}$ changes at most by $\mathcal{L}_0$. It follows that

$$\left|\delta \int_{\eta_i}^{\eta_f} \mathcal{L}_0 d\eta\right| \le \frac{|\mathcal{L}_{0\,\max}|}{N} \times \max|\Delta|. \tag{8}$$

Performing the variation of this inequality leads to Eq.(6) with the 0 replaced by a function f not larger than $|\mathcal{L}_{0\,\max}| \times \max|\Delta|/N^2$. •

In order to understand what inequality (8) means let us specialize to a case of the averaged Lagrangian $\mathcal{L}_0$ not depending explicitly on time. Then the Hamiltonian $H_0 = \boldsymbol{p}_0 \cdot \boldsymbol{v}_0 - L_0(\boldsymbol{x}_0, \boldsymbol{v}_0)$, where $L_0 = -\mathcal{L}_0(\omega - \boldsymbol{k}\cdot\boldsymbol{v}_0)$, owing to $dH/dt = \partial H/\partial t = -\partial L_0/\partial t = 0$, expresses the energy conservation $H = E = \text{const}$. A straightforward estimate shows that the uncertainty f in Eq.(6) leads to an energy uncertainty $\Delta H/H \lesssim 2\pi/N$. This means that Eq.(6) is adiabatically zero and the total cycle-averaged energy is an adiabatic invariant in the rigorous mathematical sense [7]. For $N \to \infty$ Eq.(6) becomes exact. Perturbative averaging of a Lagrangian was used in [8].

The relativistic Hamiltonian of a point charge in the electromagnetic field follows from Eq.(3),

$$H = \boldsymbol{p}\cdot\boldsymbol{v} - L = \left\{m^2c^4 + c^2(\boldsymbol{p} - q\boldsymbol{A})^2\right\}^{1/2} + \Phi, \tag{9}$$

with the canonical momentum $\boldsymbol{p} = \partial L/\partial \boldsymbol{v} = \gamma m\boldsymbol{v} + q\boldsymbol{A}$. Its numerical value is the total energy $E = \gamma mc^2 + \Phi$. Considering a monochromatic wave in vacuum we can set $\Phi = 0$. This motion is exactly solvable [9]. The cycle-averaged quiver energy in the oscillation center system is given by

$$H_0 - mc^2 = mc^2\left\{\left(1 + \frac{q^2}{\alpha m^2c^2}\hat{\boldsymbol{A}}\cdot\hat{\boldsymbol{A}}^*\right)^{1/2} - 1\right\} = W \tag{10}$$

with $\alpha = 1$ for circular and $\alpha = 2$ for linear polarization. If the effective mass $m_{\text{eff}} = -\mathcal{L}_0\gamma_0(d\eta/dt)/c^2$ is introduced, $L_0 = \mathcal{L}_0 d\eta/dt$ shows that in an arbitrary inertial frame in which the oscillation center moves at speed $\boldsymbol{v}_0$, L_0 and H_0 are those of a free particle with space and time dependent mass m_{eff},

$$L_0(\boldsymbol{x}_0, \boldsymbol{v}_0, t) = -\frac{m_{\text{eff}}c^2}{\gamma_0}, \quad H_0(\boldsymbol{x}_0, \boldsymbol{p}_0, t) = \gamma_0 m_{\text{eff}}c^2; \tag{11}$$

$$\gamma_0 = \left(1 - \frac{v_0^2}{c^2}\right)^{-1/2}, \quad p_0 = \gamma_0 m_{\text{eff}}\boldsymbol{v}_0.$$

Expressions (11) hold in any electromagnetic field in vacuum in which an oscillation center can be defined. In the special case of Eq. (10) $m_{\text{eff}} = (1 + q^2\hat{\boldsymbol{A}}\cdot\hat{\boldsymbol{A}}^*/\alpha m^2c^2)^{1/2}$.

In the oscillation center system, i.e. in the inertial frame in which at the instant t $\boldsymbol{v}_0(t) = 0$ holds, the ponderomotive force follows from Eqs.(6) and (11),

$$\boldsymbol{f}_p^N \equiv \frac{d\boldsymbol{p}_0}{d\tau} = \frac{\partial L_0}{\partial \boldsymbol{x}_0} = -c^2\boldsymbol{\nabla} m_{\text{eff}}. \tag{12}$$

The force $\boldsymbol{f}_p$ is given the index N since it is a Newton force (co-moving system); τ is the proper time. The Minkowski ponderomotive force F_p, valid in any inertial system, is

$$F_p = \left(\boldsymbol{f}_p^N + \frac{\gamma_0 - 1}{v_0^2}(\boldsymbol{f}_p^N\cdot\boldsymbol{v}_0)\boldsymbol{v}_0,\ \ \frac{\gamma_0}{c}\boldsymbol{v}_0\cdot\boldsymbol{f}_p^N\right). \tag{13}$$

Hence, the three-dimensional relativistic ponderomotive force $\boldsymbol{f}_p$ at any oscillation center speed $\boldsymbol{v}_0$ is the Einstein force,

$$\boldsymbol{f}_p = -\frac{c^2}{\gamma_0}\left\{\boldsymbol{\nabla}^N m_{\text{eff}} + \frac{\gamma_0 - 1}{v_0^2}(\boldsymbol{v}_0\cdot\boldsymbol{\nabla}^N m_{\text{eff}})\boldsymbol{v}_0\right\}. \tag{14}$$

In the non-relativistic limit Eq.(2) is easily recovered.

To see the power of the Lagrangian formulation, Eq.(6), we calculate $\boldsymbol{f}_p$ in a non-relativistic Langmuir wave of the form $E(x,t) = \hat{E}(x,t)\sin(kx - \omega t)$ with slowly varying amplitude $\hat{E}$. In lowest order the potential is $\Phi(x,t) = (\hat{E}/k)\cos(kx - \omega t)$ and

$L = mv^2/2 - q\Phi$. In the frame comoving with x_0 the particle sees the Doppler-shifted frequency $\Omega = \omega - kv_0$ (plus higher harmonics which are not essential here). With the periodic excursion $\zeta(t)$ around x_0 the potential is $\Phi(x,t) \simeq \Phi(x_0,t) + \zeta(t)\partial\Phi/\partial x_0$. From this $L_0 = mv_0^2/2 - \alpha\hat{E}^2/\Omega^2$, $\alpha = q^2/4m$, results in lowest order. With this Lagrangian it follows from Eq.(6) for $\hat{E} = \hat{E}(x)$ (no explicit time dependence) that

$$f_p = m\frac{dv_0}{dt} = -\alpha\frac{(1-V_0)(1-3V_0)}{\omega^2(1-V_0)^4 - 6\alpha\hat{E}^2/mv_\varphi^2}\frac{\partial}{\partial x}\hat{E}^2. \tag{15}$$

In the last expression V_0 is the oscillation center velocity normalized to the phase velocity $v_\varphi = \omega/k$, $V_0 = v_0/v_\varphi$. The formula shows that f_p changes sign when the particle is injected into the Langmuir wave with a velocity v_0 exceeding $v_\varphi/3$. In regions where the standard expression for f_p, Eq.(2), always exhibits repulsion the more exact treatment can lead to attraction. Eq. (15) was also derived in a more formal but physically less transparent manner in [6]. Uphill acceleration in an electron plasma wave of increasing amplitude $\hat{E}(x)$ is confirmed by the numerical solution of the exact equation of motion (Fig.1a). If $\hat{E}(x)$ grows indefinitely the exact ponderomotive force changes sign again and the particle stops and is finally reflected; the corresponding path in phase space exhibits a hysteresis (Fig.1b). Uphill acceleration, occasionally observed in other context [10], is a general ponderomotive phenomenon.

Strong gradients of amplitude and, as a consequence, large ponderomotive forces appear when two or more waves superpose. Of particular importance is the case of a standing, or partially standing wave. We have numerically studied the secular motion in the field given by the vector potential

$$\boldsymbol{A}(x,t) = \hat{A}\boldsymbol{e}_y(\sin\eta_+ - \sin\eta_-), \quad \eta_\pm = kx \pm \omega t. \tag{16}$$

For field amplitudes $\xi \leq 0.1$ (non-relativistic case), $\xi = |q|\hat{A}/mc$, splitting of the motion into a fast and a secular, i.e. ponderomotive one, makes sense. In Fig. 2a an electron orbit is followed over 110 laser cycles in the standing wave of strength $\xi = 0.1$: the motion is regular and its dependence on the phase of the wave field is weak (narrow band of orbits). The corresponding Nd laser intensity ($\omega_{\mathrm{Nd}} = 1.78\times10^{15}\ \mathrm{s}^{-2}$) is $I_{\mathrm{Nd}} = 1.21\times10^{16}\ \mathrm{Wcm}^{-2}$. At $\xi = 0.25$ ($I_{\mathrm{Nd}} = 7.6\times10^{16}\ \mathrm{Wcm}^{-2}$) some electrons starting near the maximum $A(x) = 2\hat{A}$ are able to escape from the ponderomotive potential well; the secular motion through the well exhibits a strong phase dependence. At $\xi = 0.5$ ($I_{\mathrm{Nd}} = 3\times10^{17}\ \mathrm{Wcm}^{-2}$) the motion becomes totally chaotic (see Fig. 2b): slight changes in the initial time produce totally different orbits, a clear signature of chaos. The chaotic motion has its origin in the Doppler effect since the moving electron "sees" one wave as blue- and the other one as red-shifted. No oscillation center exists under such circumstances and a secular time scale may only build up on the statistical average.

Electrons in a dense plasma behave differently since they are coupled to the massive ions by an ambipolar electric field E_s. In Fig. 3 the calculation of Fig. 2 is repeated for $\xi = 0.5$ in a plasma of which the density is assumed to be such as to keep the oscillation center in a steady state position. In Fig. 3a the single arc-like (no longer 8-shaped) orbits are shown. The inclusion of E_s in the equation of motion is essential for producing the regular orbits and the correct ponderomotive forces (Fig. 3b). For comparison the bare dotted line is the ponderomotive force from Eq.(2) without including the space charge field E_s in f_p. We estimate from numerical runs that beyond $I_{\mathrm{Nd}} = 10^{18}$ Wcm^{-2} no regular ponderomotive force exists in the dense plasma either.

We conclude as follows. (i) When an oscillation center of motion exists the invariant cycle-averaged Lagrangian describes the ponderomotive motion in arbitrarily strong fields. (ii) The ponderomotive force in a monochromatic travelling, locally plane wave of arbitrary strength in any reference system can be expressed analytically. (iii) In a longitudinal wave uphill acceleration and phase space-hysteresis may occur. Finally, (iv) superposition of different modes of the same frequency leads to a limiting intensity above which transition to chaos occurs. The influence of dissipation (radiation losses, friction) on the ponderomotive force is also well understood now, but will be treated in a separate paper.

*) On leave from Rand Afrikaans University, Johannesburg, South Africa.

REFERENCES

[1] M. Tabak, J. Hammer, M.E. Glinsky, W.L. Kruer, S.C. Wilks, J. Woodworth, E.M. Campbell, M.D. Perry, and R.J. Mason, Phys. Plasmas **1**, 1626 (1994).

[2] L.D. Landau and E.M. Lifshitz, *Mechanics*, Pergamon Press, Oxford, 1976, p. 93. H.A.H. Boot, S.A. Self and R.B.R. Shersby-Harvie, J. Electron. Control **4**, 434 (1958). A.V. Gapunov and M.A. Miller, Sov. Phys. JETP **7**, 168 (1958). T.W.B. Kibble, Phys. Rev. **150**, 1060 (1966). F.A. Hopf, P. Meyestre, M.O. Scully and W.H. Louisell, Phys. Rev. Letters **37**, 1342 (1976).

[3] G. Schmidt, *Physics of High Temperature Plasmas*, Academic Press, New York, 1979, p. 47-50.

[4] G.G. Grebogi and R.G. Littlejohn, Phys. Fluids **27**, 1996 (1984).

[5] J.R. Cary and A.N. Kaufman, Phys. Fluids **24**, 1238 (1981).

[6] B. Weyssow and R. Balescu, J. Plasma Physics **37**, 467 (1987).

[7] V.I. Arnold, *Dynamical Systems III*, Springer Verlag, Berlin, 1988, p.200. W.-H. Steeb, *A Handbook of Terms Used in Chaos and Quantum Chaos*, BI, Mannheim, 1991, p. 3.

[8] G.W. Kentwell, J. Plasma Physics **34**, 289 (1985).

[9] L.D. Landau and E.M. Lifshitz, *The Classical Theory of Fields*, Pergamon Press, Oxford, 1980; p. 118. E.S. Sarachik and G.T. Schappert, Phys. Rev. D **1**, 2738 (1970).

[10] K. Morawetz and A.P. Jauho, Phys. Rev. E **50**, 474 (1994).

FIGURES

FIG. 1. Ponderomotive motion of an electron ($q = -e$) in a travelling Langmuir wave. In (a) the velocity $V = v/v_\varphi$, $v_\varphi = \omega/k$, is shown as a function of position $X = kx$ in the longitudinal field $\xi(1 - \exp(-0.1X))\sin(X - T)$, $\xi = e\hat{E}/m\omega v_\varphi = 0.1$, for the initial conditions $X_0 = 0$, $V_0 = 0.6$ (trajectory a). The oscillation center motion from Eq. (2) (dotted line b) shows a slight decrease, whereas the secular acceleration by Eq. (15) (dotted line c) is in good agreement with that resulting from trajectory a. The lower curve d shows the harmonic electric field as "seen" by the moving electron. In (b) the normalized kinetic energy $V_0^2/2$ is shown as a function of $\Phi_p/m_e v_\varphi^2$ from Eq. (2) for the linearly increasing field $2.5 \times 10^{-3}\xi X \sin(X - T)$, $\xi = 1$, and injection velocities $V_0 = 1/3$ (lower curves) and $V_0 = 0.43$ (upper curves). The motion shows a pronounced hysteresis in phase space owing to different acceleration in co- and counter-motion.

FIG. 2. Regular (a) and stoachstic motion (b) over 110 laser cycles of an electron placed with oscillation center speed $v_0 = 0$ at the position $X = kx_0 = 39\pi/40$ in a plane monochromatic standing wave; ordinate $Y = ky$ points into field direction. In (a) the maxima of the ponderomotive potential Φ_p are located at $X = 0$, π; at $X = \pi/2$ $\Phi_p = 0$; normalized amplitudes of counterpropagating waves are $\xi = e\hat{A}/mc = 0.1$. The electron motion evolves in a narrow band between the potential maxima. Band broadning around $X = \pi/2$ is due to Doppler effect. In (b) Φ_p (dashed line) is 25 times stronger ($\xi = 0.5$), the electron motion is erratic, sweeping over 21 maxima of Φ_p during 110 cycles. Note also the enormous transverse excursion of $\Delta y = 0.9$ wavelengths ($\Delta Y = 5.8$).

FIG. 3. Electron orbits and ponderomotive potential in a standing plane, monochromatic wave in a uniform plasma. (a) Electron orbits around oscillation center tied to the ions by the induced ambipolar field; field distribution as in Fig. 2(a), field strength $\xi = 0.5$ as in Fig. 2(b). In (b) the segments parallel to $X = kx$ indicate the orbit widths in X-direction; the connecting dotted line indicates the relativistic ponderomotive force. For comparison, the bare dotted line is f_p from Eq. (2); the field is given in dimensionless units of $eE/m\omega c$.

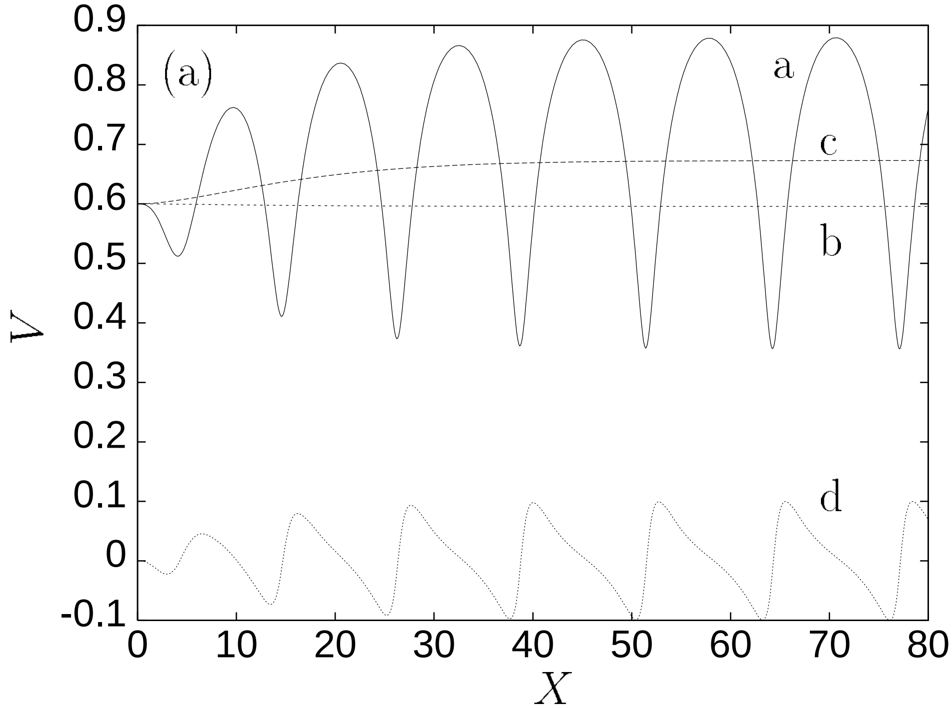
(a)
a
c
b
d
V
X
0.9
0.8
0.7
0.6
0.5
0.4
0.3
0.2
0.1
0
-0.1
0
10
20
30
40
50
60
70
80

Fig. 1a

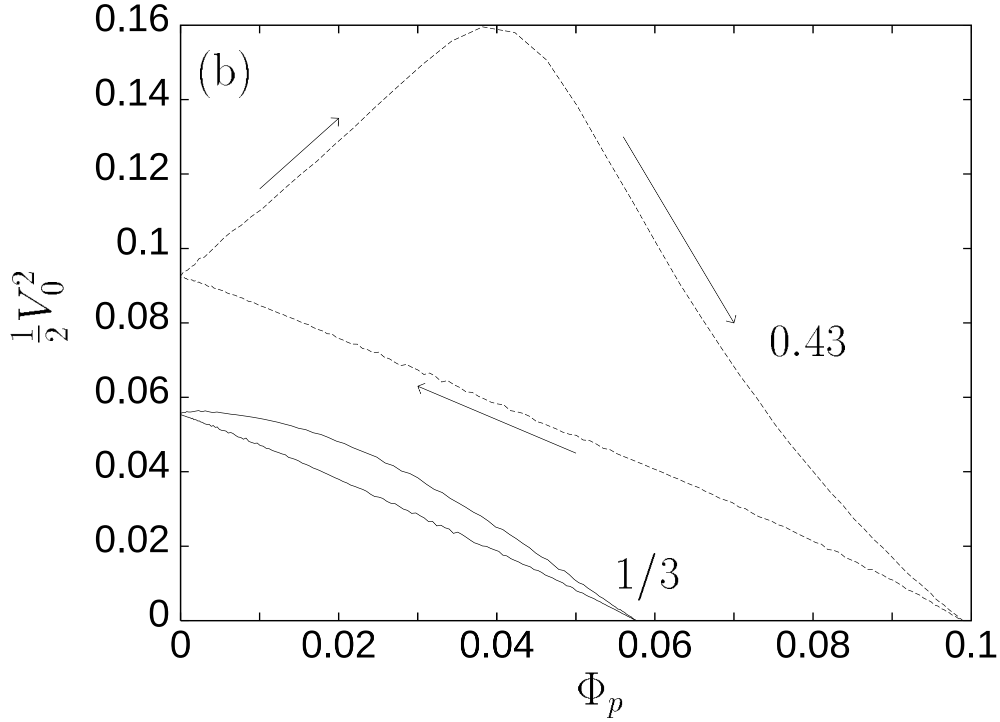
(b)
0.43
1/3
$\frac{1}{2}V_0^2$
Φ_p
0.16
0.14
0.12
0.1
0.08
0.06
0.04
0.02
0
0
0.02
0.04
0.06
0.08
0.1

Fig. 1b

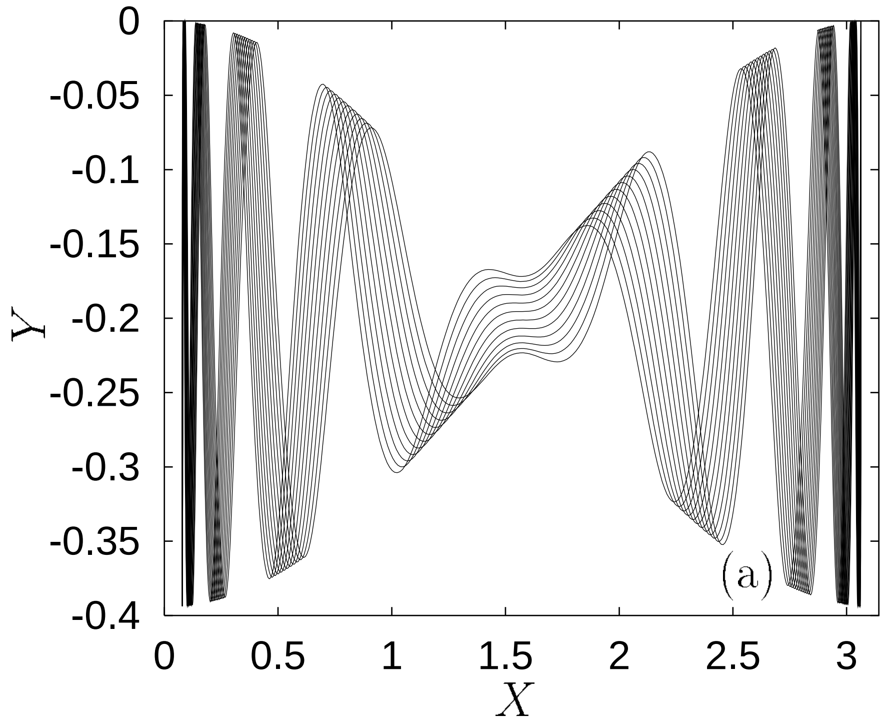

0
-0.05
-0.1
-0.15
-0.2
-0.25
-0.3
-0.35
-0.4
Y
0
0.5
1
1.5
2
2.5
3
X
(a)

Fig. 2a

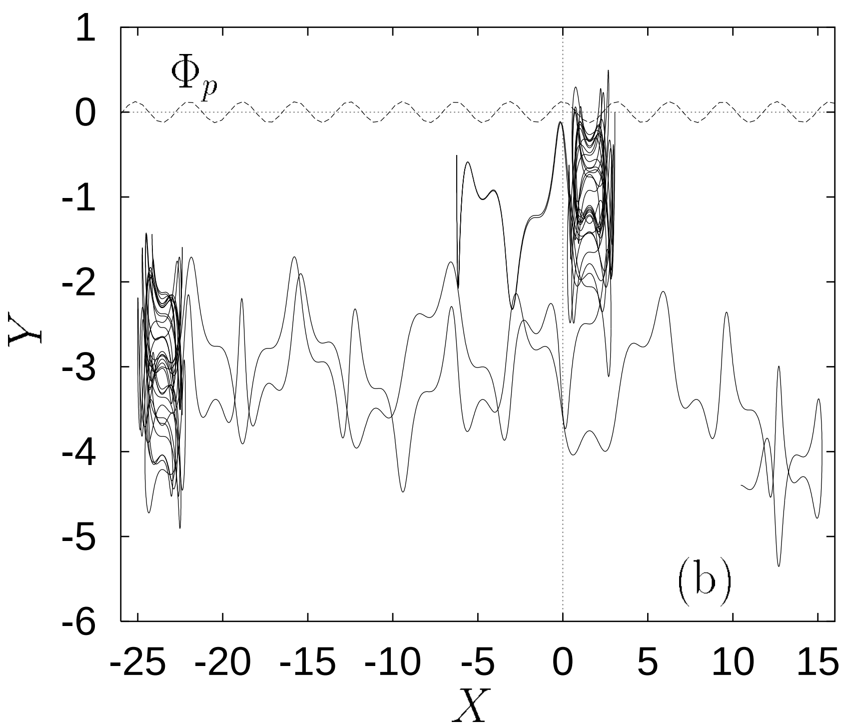

1
0
-1
-2
-3
-4
-5
-6
Y
Φ_p
(b)
-25
-20
-15
-10
-5
0
5
10
15
X

Fig. 2b

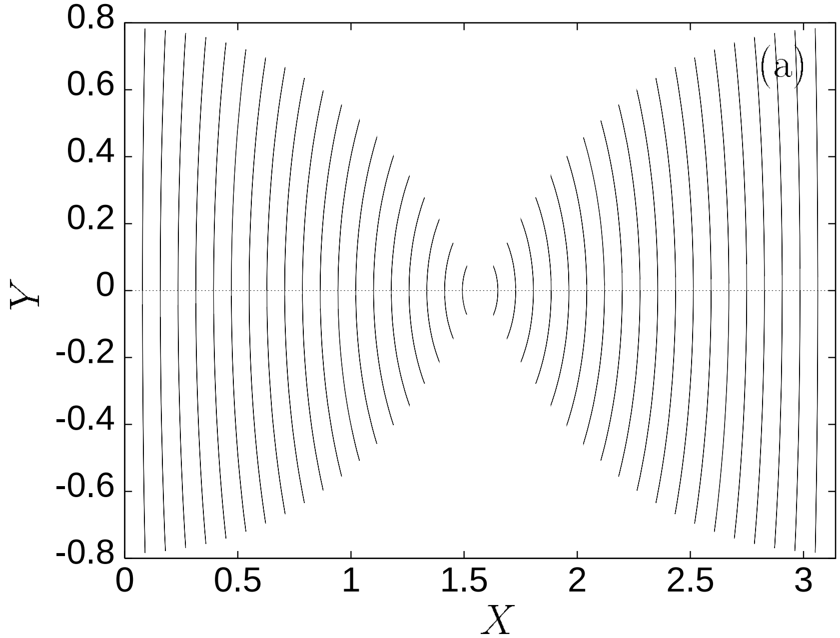
0.8
0.6
0.4
0.2
0
-0.2
-0.4
-0.6
-0.8
Y
0
0.5
1
1.5
2
2.5
3
X
(a)

Fig. 3a

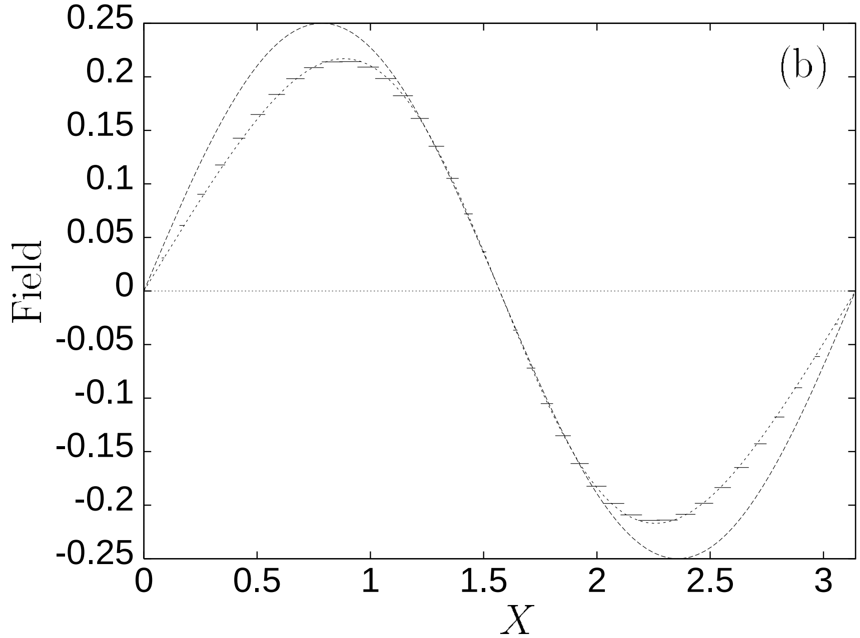
0.25
0.2
0.15
0.1
0.05
0
-0.05
-0.1
-0.15
-0.2
-0.25
Field
0
0.5
1
1.5
2
2.5
3
X
(b)

Fig. 3b